Torsional Correlates for End Systolic Volume Index in Adult Healthy Subjects

Concetta Torromeo

Antonietta Evangelista

Michele Schiariti

Paolo Emilio Puddu

Department of Cardiovascular
Respiratory, Nephrological
Anesthesiological and Geriatric Sciences
Sapienza University of Rome
Policlinico Umberto I, 00161 Rome
Italy

Natesa G. Pandian
Cardiovascular Imaging and Hemodynamic Laboratory
Tufts Medical Center
Boston (MA)
USA

Paola Nardinocchi
Dipartimento di Ingegneria Strutturale e Geotecnica
Sapienza University of Rome
Rome
Italy

Valerio Varano

Stefano Gabriele

Luciano Teresi

LaMS, Modeling & Simulation Lab
Università degli Studi Roma Tre
Rome
Italy

Paolo Piras
Department of Cardiovascular
Respiratory, Nephrological
Anesthesiological and Geriatric Sciences
Sapienza University of Rome
Policlinico Umberto I, 00161 Rome
Italy

Dipartimento di Scienze
Università Roma Tre
Rome, Italy

Center for Evolutionary Ecology
Rome
Italy

Abstract

3-dimensional (3D) speckle tracking-based motion-detecting echocardiography (STE) was used in order to evaluate left ventriculum (LV) rotation, twist and torsion in 16 segments (base, medium, apex and global) in 32 healthy subjects. All parameters were indexed by body surface area. Then, gender-related differences were removed by gender-centering the entire dataset. Linear models were run to predict ESVI by using single torsional parameters and by evaluating the degree of their collinearities. Given the strong collinearities on predictors, we performed a principal component regression and we found an axis that predicts ESVI better than the single most correlated original variables. We statistically assessed that this axis is a significant best predictor of ESVI than original torsional variables yet containing strict relationships with them. The physiological implications of our results are discussed in the context of heart contractility theory as well as of the actual difficulties to measure electro-mechanical determinants of healthy subjects in vivo.

Keywords: Left Ventriculum, ESVI, Torsional parameters, PCA regression, healthy subjects

1. Introduction

Left ventricular (LV) pumping function is associated with rotational movements, radial thickening, circumferential strain and longitudinal shortening (Sengupta et al., 2008). LV twist or torsional deformation during systole is the consequence of apical rotating counter-clockwise whereas basal segments concomitantly rotate clockwise, which has long been interpreted as a powerful co-generator of systolic efficiency (Shaw et al., 2008; Kim et al., 2009). The morphological basis rests on the ventricular muscle helical-band theory as a comprehensive mechanistic interpretation of LV rotation or twist (Corno et al., 2006; Buckberg et al., 2008; Grosber and Gharib, 2009; Nasiraei-Moghaddam and Gharib., 2009) . Earlier, Streeter et al. (1969) found that fiber-angle changing from endo- to epi-cardium might be crucial to explain LV twist, an anatomical observation which was more recently refreshed by sophisticated animal studies (Smerup et al, 2009). We considered transparietal fiber crossing with well-defined angles and transmural gradients of contractile state, based on differential action potential durations and showed that these have a definite role (Evangelista et al., 2011) and may well contribute to lower energetic expenditures and thus increased efficiency (Nardinocchi et al., 2012). On the other hand, when rotation is absent or reduced, ejection fraction (EF) is most frequently lower than normal, even with high radial strain (which entails radial thickening) and longitudinal shortening (which is accompanied by higher longitudinal strain; Park et al., 2012). Moreover, LV unscrewing in diastole, adding to LV twist in systole, may influence global performance and might concomitantly be used to assess overall LV function (Buckberg et al., 2011).

Recent advances in cardiac imaging enabled to quantify cardiac motion noninvasively: 3-dimensional (3D) speckle tracking-based motion-detecting echocardiography (STE) was tested in computing LV twist and was validated by invasive sonomicrometry (Zhou et al., 2010; Ashraf et al., 2010). 3DSTE imaging allows for an objective and quantitative evaluation of global and regional myocardial function independently from the insonation's angle and from cardiac translational movements and it is therefore, at least theoretically, better than 2-dimensional STE (Kim et al., 2007; Pérez et al., 2009; Maffessanti et al., 2009; Sun et al., 2012). Several studies pointed to a significant correlation between LV torsion and EF when the aim was at assessing clinically LV systolic function (Kim et al., 2007; Uznańska et al., 2008). However, in vigil humans there is a lack of investigations whereby 3DSTE was tested as a potential predictor of LV function (and/or contractile state).

End-systolic volume index (ESVI) and LV contractile state have an inverse relation at rest and after exercise, or following inotropic interventions (D'Agostino et al., 1983; Higginbotham et al., 1986; Grosu et al., 2005): thus it might be speculated that ESVI may represent an interesting and simple noninvasive tool to assess contractility (i.e. the inherent capacity of the myocardium to contract independently of changes in pre-load and/or after-load) in humans (Evangelista et al., 2011; ,Grosu et al., 2005; Suga et al., 1973; Sagawa et al., 1977). We hypothesized that LV torsional parameters (twist, rotation or torsion *sensu strictu*) may predict ESVI. This study aims at determining whether LV torsional deformation ascertained by primary and/or secondary parameters derived from 3DSTE could be used as noninvasive, quantitative predictors of ESVI in vigil healthy subjects.

2. Material and Methods

2.1. Study Population

The study was conducted after approval of the **"**Dipartimento di Scienze Cardiovascolari, Respiratorie, Nefrologiche, Anestesiologiche e Geriatriche, Sapienza-Università di Roma" review board, and was performed in accordance with the ethical guidelines of the Declaration of Helsinki. Written informed consent was obtained from each of the 32 healthy volunteers that were randomly selected from the local list of employees at a single University Hospital Department. They were solicited for participation which was agreed by 95% of invited individuals. Individuals were subjectively healthy without a history of hypertension or cardiac disease and were not taking medications. They all had normal ECG and blood pressure below 140/90 mmHg. They all gave informed consent in accordance to local ethical standards.

2.2. Equipment

Echocardiographic examinations were performed with an Aplio-Artida ultrasound system (Toshiba Medical Systems Co, Tochigi, Japan). Full-volume ECG-gated 3D data sets were acquired from apical positions using a 1-4 MHz 3D matrix array transducer to visualize the entire LV in a volumetric image. To obtain these 3D data sets, four or six sectors were scanned from consecutive cardiac cycles and combined to provide a larger pyramidal volume covering the entire LV. Sector width was optimized to allow for complete myocardial visualization while maximizing the frame rate. Mean volume rates were 20 ± 2 volumes/s in the apical views for gray scale imaging used for 3D speckle tracking analysis.

2.3. Technique

Each 3D data set was displayed in a 5-plane view: (A) an apical 4-chamber view; (B) a second apical view orthogonal to plane A; and (C) 3 short-axis planes: in the apical, midventricular and basal portions of the left ventricle, respectively (Figure 1). The user then set three markers on planes A and B; in each plane, one marker was set at the apex and the other two at the edges of the mitral valve ring. The software then detected the LV endocardium, and the user set a default thickness for the myocardium. After the markers had been selected, the system performed the wall motion-tracking analysis through the entire cardiac cycle. The LV was divided into 16 segments (6 basal, 6 mid-LV, and 4 apical) on the basis of the American Heart Association standards for myocardial segmentation (Cerqueira et al., 2002), and each segment was individually analyzed (Figure 2). The results of the 3D-wall motion analysis were presented to the user as averaged values for each segment in each frame of the cardiac cycle generating time-curves graphs. For each consecutive time frame, LV volume was calculated by voxel count inside the detected endocardial border. End-diastolic volume (EDV) and end-systolic volume (ESV) were then obtained from the LV volume curve as the respective maximum and minimum values, concurrently providing the calculated EF and LV mass (Nesser et al., 2009; Kleijn et al., 2012). All variables were normalized by dividing by body surface area (using the formula by BuBois and DuBois: [weight$^{0.425}$ x height$^{0.725}$] x 0.007184) (Cameli et al., 2011). The parameters considered and briefly categorized here are exclusively those related to torsion *sensu latu*, being longitudinal and circumferential strain parameters directly related to indexed ESV (ESVI) as derived from volumetric contraction. Relating strain parameters to ESVI represents a circular rationale in our primary hypothesis that is focused solely on LV torsion. Thus, we consider these parameters (Maffessanti et al., 2009; Evangelista et al., 2009; Geyer et al., 2010).

Rotation**:** is the movement that the ventricle does around the longitudinal axis and is expressed in degrees. For counter-clockwise rotation, which normally occurs at the apex level, there are a certain amount of positive degrees. Generally the base presents a clockwise rotation which is expressed either by 0° rotation or few negative degrees.

Twist and Torsion: LV twist is a component of the normal LV systolic contraction that arises from the reciprocal rotation of the LV apex and base during systole and constitutes an important aspect of cardiac biomechanics. LV twist is calculated as the net difference in mean rotation between the apical and basal levels and it is expressed in degrees. LV torsion is defined as LV twist normalized by the base-to-apex distance which is expressed in degrees/cm. Accordingly, twist and torsion are not synonymous.

2.4. Statistical Analysis

All analyses were performed in R statistical software. A random sample of 9 subjects was chosen to assess repeatability among selected primary variables.

Apex and global rotations were again calculated by the same observer who processed the acquired images several months apart the initial measurements, by running again the Aplio-Artida calculation software. Standard formulae were used based on absolute differences normalized by actual average values between the 2 measurements and the result was percentage measurement error.

Gender related differences was removed by subtracting (for all variables intervening in our study) to any entry the corresponding per-gender mean. This is a common strategy when gender differences are not under investigation (Mitteroecker et al., 2012).

As first, the independent determinants of ESVI were explored by single linear regressions using ESVI as dependent and torsional parameters as independents. We also evaluated the degree of collinearity in our predictors by computing the variance inflation factor of a multiple regression model including all predictors. We anticipate here that we found serious collinearities in our independent table. Thus, we adopted a common strategy in presence of strong collinearities among predictors: we first performed a principal component (PC) analysis (PCA) on predictors in order to eliminate any collinearity and to find orthogonal axes of maximal variation. Then, using all non zero PCs, we selected PC(s) maximally correlated with our dependent variable, i.e. ESVI. This is aimed at finding, if any, vector(s) able to predict ESVI better than single original predictors. We note that we performed PCs selection by including in our analysis even those PCs explaining a small fraction of total variance. This vision traces back to the seminal paper of Joliffe (1982) that demonstrated that, when used as regressors, even PCs explaining small portions of variance can be better predictors than those bearing larger variances. It happens because the PCA machinery performed on predictors does not care of their correlation with an external variable. Thus, the component(s) most correlated with a dependent variable can be at any variance rank position of PC scores. The selection of PCs was performed using two different methods: the classical stepwise regression (using step() function in R package "base", R Core Team, 2013) and the method "BIOENV" firstly proposed by Clarke and Ainsworth (1993) using bioenv() function in R package "vegan" (Oksanen et al., 2013).

The former method is widely used and is based on regression theory and uses the Akaike Information Criterion (AIC) for including/excluding independent variables. The latter is based on the dissimilarity matrix computed in both dependent and independent table. Then it selects all possible subsets of independent variables, scales the variables, and calculates Euclidean distances for this subset. It finds the correlation between dependent dissimilarities and independent distances, and for each size of subsets, saves the best result. The subset with higher correlation is the best one. This strategy has the advantage that there is no specific direction (backward or forward) for including independent variables in the model. After the selection of the best PC(s) predictors(s), we performed two regression models, one with the original predictor(s) variables found significant and another with PC(s) found significant. The two models have been compared not only by evaluating the R-squared and the AIC (that allow a qualitative evaluation of the difference between the two models), but also using the Davidson-MacKinnon J test using function jtest() of R package "lmtest". While AIC measures the amount of information lost during model construction, the J test is aimed at assessing the statistical significance of the difference between two non nested regression models. The rationale behind Davidson-MacKinnon J test is that if the first model contains the best set of regressors, then including the fitted values of the second model into the set of regressors should provide no significant improvement. But if it does, it can be concluded that the first model does not contain the best set of regressors. Significance level was set at 0.05.

3. Results

A total of 32 healthy subjects were enrolled. Apex and global LV rotations, among the primary variables, presented the largest average values and were thus selected to test repeatability which did not exceed 29%. Table 1 shows descriptive statistics for variables included in our dataset.

Table 2 shows results for single regressions between ESVI and torsional parameters. Rotation base is the sole parameter that significantly predicts ESVI. Fig. 3 shows regression line and confidence intervals for this relationship while Table 3 shows the results of this regression model, Normality test on residuals (Lilliefors test), autocorrelation test (Durbin-Watson test) and heteroskedasticity test (Breusch-Pagan test) were all non significant. Variance inflation factor is huge for all independent variables in a multiple regression model including all 12 predictors (range: 2088.942 to 624499.818). For this reason we performed a PC analysis on torsional parameters table. Table 4 shows the variance explained by all non zero PCs.

Stepwise regression (using "both directions" option) identified the PC4 as the sole significant predictor of ESVI among all non zero PCs. The same result has been found by applying the bioenv() procedure described above. Fig 4 and Table 5 show the results and confidence intervals for the regression model with ESVI as dependent and PC4 as independent. AIC is smaller for the second regression model and the R-square is sensibly higher. The J test is significant if the predicted values of the second model are added to the first one, while it is not significant for the opposite. These evidences clearly suggest that PC4 is a significantly best predictor of ESVI relatively to Rotation base alone. The biological meaning of PC4 is mainly driven by Rotation base, as expected. In fact, Rotation base is the sole original variable significantly associated to ESVI. However, being PCs linear combinations of the entire set of predictors, any PC axis inherits the contribution of all predictors that in our case are strongly collinear. Thus, a PC analysis could lead to axes that alone could be better descriptors of ESVI. PC4 is correlated also with Twist base and Torsion base as it can be seen in the biplot shown in Fig. 5. Table 6 shows, instead, the correlation coefficients between torsional parameters and ESVI or PC4 corresponding to Fig. 5.

4. Discussion

General Results

Our results indicate that torsional deformation *sensu latu* is a significant predictor of ESVI and thus deserves attention *in vivo*. The results from the present study conceptually agree with those of Sun et al. (2012) and Cameli et al. (2011), both concentrated in LV torsional deformation as a dependent rather than an independent variable. Using 2DSTE, respectively 228 (109 males, mean age 44±15years, ranged 18-78 years) and 119 healthy subjects were investigated at rest. Older age rather than gender increased global LV rotation and twist (Sun et al., 2012). On the other hand, LV twist was predicted (in a stepwise linear regression model) by ESVI (β= -0.200, $P<0.0001$), peak early diastolic mitral annulus velocity (β= -0.186, $P = 0.0001$), heart rate (β= 0.178, $P=0.0003$), and male gender (β= -0.174, P=0.0004) with similar results found in relation with LV torsion. However, there was only 11-26% of variability explained by regression parameters and the conclusion was that conventional echocardiographic and clinical variables are not able to predict LV torsion mechanics (Cameli et al., 2011).

In our study we related gender and body mass adjusted ESV to torsional parameters as measured by 3DSTE. We stressed our hypothesis by eliminating collinearities in predictors and we found that PC analysis is a very useful tool to extract axes able to predict ESVI better than original variables. We underline that PCA regression is essential to handle the entire set of torsional variables and we suggest to adopt it in future studies involving the same set of parameters. We also recommend to evaluate *all* non zero PCs during regressor selection. The rotation_base is undoubtedly the most important variable in explaining ESVI but also torsion_base and twist_med are important, as it can be seen in Fig. 5. Interestingly, all these variables describe and/or contribute to LV torsional deformation.

In future investigations it will be important to test the intra and inter-observer variabilities of the parameters measured by 3DSTE, not just apex and global LV rotations as performed here. Indeed, a variability of slightly less than 30% for repeated measures might be a significant limitation factor to the optimal development of this technique.

From Anatomy to Function

The mechanistic basis for the twisting/torsional motion lies in the complex LV spiral architecture as shown by the anatomical studies of Francisco Torrent-Guasp (Corno et al., 2006; Buckberg et al., 2008; Grosber and Gharib, 2009; Nasiraei-Moghaddam and Gharib., 2009; Buckberg et al., 2011). The normal heart has a helical formation whereby the fiber orientation has an oblique angle from the mid ventricle to the apex, an observation dating back to Richard Lower's anatomical investigations as early as 1669. Viewed from the apex, left-handed epicardial fiber helix tries to pull the apex counterclockwise and the base clockwise (Sengupta et al., 2008). The right-handed helix in the endocardium does the opposite; however, because the epicardium is farther from the centerline, its torque is greater and thus it dominates the twisting (Evangelista et al., 2011; Nardinocchi et al., 2012). Arts' group (Vendelin et al., 2002) demonstrated that systolic twist tends to equalize transmural fiber stress and strain in the thick-walled LV chamber, thereby reducing transmural gradients of myofiber work and oxygen consumption. Hansen et al. (1991) showed that LV torsion depends mainly on the strength of contraction and LV fiber architecture, and it is independent of the load conditions. Quantification of LV torsion may thus provide a sensitive and relatively load-independent measure of contractile performance and may prove to be useful in serial assessment of LV function (Kim et al., 2009).

Local variations contribute importantly to deformation (Corno et al., 2006; Buckberg et al., 2008; Grosber and Gharib, 2009; Nasiraei-Moghaddam and Gharib., 2009; Buckberg et al., 2011) : the endocardium contributes predominantly to longitudinal shortening, the meso and epicardium respectively produce the circumferential deformation and LV rotation whereas all three layers contribute to radial thickening. The helical movement of the myocardium provides a further mechanistic explanation for its screwing movement during the mechanical cycle. Indeed, during ejection, the epicardium, which has one arm longer than the helix of the endocardium, determines the direction of global rotation: counterclockwise rotation of the apex and clockwise rotation of the base Sengupta et al (2006).

However, all the abovementioned pathophysiological considerations await future studies to assess cause and effect relationships between torsional deformation and ESVI as a dependent variable.

The Elusive Concept of Contractility

The systolic ventricular myocardial function can be defined as the ability of the ventricle to enter a certain volume of blood per unit of time at a certain pressure in the circulation (Evangelista et al., 2011). In the heart *in situ*, changes in pre-load, after-load or contractility may affect the levels of cardiac output through indirect changes of the other parameters and it is often difficult to extrapolate the effects on pump function of changes in each individual factor (Bombradini, 2005). Energetically, contractility is expressed as the sum of the components of load-independent ventricular work: expulsion and internal works. However, it is difficult to estimate the intrinsic contractile properties of cardiac muscle *in vivo*. In fact, it is only in presence of constant load, synchronous contraction and a stable heart rate, that a change in myocardial performance may be considered to express a variation of inotropism (D'Agostino et al., 1983; Higginbotham et al., 1986; Grosu et al., 2005). Ethically, it is difficult, if not impossible, to imagine using direct invasive means to measure contractility by independent variables, in healthy humans.

ESVI: A Load-Independent Index of Contractility?

The idealized contractility is expressed in the isolated heart as the maximal velocity of contraction of unloaded muscle fibers (Vmax). This value is defined as the maximal velocity of contraction, when there is no load on the isolated muscle (Evangelista et al., 2011; Bombardini, 2005). Although Vmax is a strictly preload- and after-load-independent index, thus fulfilling the theoretical requirements for contractility quantification, it is not possible to use it *in vivo*. In sake of surrogate parameters, Suga and Sagawa (Suga et al., 1973; Sagawa et al., 1977) measured pressure/volume loops in the intact heart. During a positive inotropic intervention, the pressure volume loop reflected smaller end-systolic volume and higher end-systolic pressure; the slope of the pressure volume relationship moved upward and to the left and became the most reliable index for assessing myocardial contractility at rest in the intact circulation, an almost insensitive parameter to changes in pre-load and after-load. Although these measures were obtained in conscious dogs, a reasonably linear relation between end-systolic pressures and end-systolic diameters (directly related to ESVI) in a given contractile state was seen: the left upper corner of the pressure-diameter loops falled on or near a rectilinear curve (Suga et al., 1973; Sagawa et al., 1977) .

Limitations and Future Directions

Only one observer was involved to obtain the digitization of 3DSTE images which may have introduced some elements of bias. The intra-observer variability seen for selected variables needs be extended to other variables and the inter-observer variability assessed. Sample size calculations were not performed since the study was conducted on a voluntary basis. The variance of the assessed parameters may be useful to calculate larger samples in future studies. Larger ranges of heart rate and fitness may also be considered.

Because LV torsion is directly related to fiber orientation (*the anatomical pre-requisite*), it might depict subclinical abnormalities in heart function and/or efficiency (Evangelista et al., 2011; Nardinocchi et al., 2012; Piras et al, 2014). There is now wide acceptance that echocardiography, especially 3DSTE may represent a new noninvasive standard (*the method*) to investigate torsion (*the physiological protagonist*) and the modifications that different conditions, from fitness to pathology, may induce on it (Sengupta et al., 2008; Shaw et al., 2008; Kim et al., 2009; Piras et al., 2014) although it will be important to ascertain whether these are compensatory or primary elements in the pathophysiological evolution.

It will be important to investigate, in large groups of individuals, not only how twist/torsion mechanics contribute to predict ESVI at rest, but also to assess (*the future*) this when different conditions such as exercise, fever and/or stress modify the heart rate/contractile relation (Bowditch effect; Grosu et al., 2005; Russel et al., 2005) to see whether period/tension relation may be reconciled, by integrating twist/torsion, with the length/tension relation so uniformely accepted to define contractility. This may hopefully increase outcome prediction and/or drive physiologically based therapies.

Acknowledgment

References

Ashraf, M., Myronenko, A., Nguyen, T., Inage, A., Smith, W., Lowe, R.I., Thiele, K., Gibbons Kroeker, C.A., Tyberg, J.V., Smallhorn, J.F., Sahn, D.J. & Song, X. 2010. Defining left ventricular apex-to-base twist mechanics computed from high-resolution 3D echocardiography: validation against sonomicrometry. Journal of the American College of Cardiology Carciovascular Imaging, 3, 227-234. (doi: 10.1016/j.jcmg.2009.09.027)

Bombardini, T. 2005. Myocardial contractility in the echo lab: molecular, cellular and pathophysiological basis. Cardiovascular Ultrasound, 3, 27. (doi:10.1186/1476-7120-3-27)

Buckberg, G., Hoffman, J.I.E., Nanda, N.C., Coghlan, C,, Saleh, S. & Athanasuleas, C. 2011. Ventricular torsion and untwisting: further insights into mechanics and timing interdependence: a viewpoint. Echocardiography, 28, 782-804. (doi: 10.1111/j.1540-8175.2011.01448.x.)

Buckberg, G., Mahajan, A., Saleh, S., Hoffman, J.I. & Coghlan, C. 2008. Structure and function relationships of the helical ventricular myocardial band. Journal of Thoracic and Cardiovascular Surgery, 136, 578-589. (doi: 10.1016/j.jtcvs.2007.10.088)

Cameli, M., Ballo, P., Righini, F.M., Caputo, M., Lisi, M. & Mondillo, S. 2011. Physiologic determinants of left ventricular systolic torsion assessed by speckle tracking echocardiography in healthy subjects. Echocardiography, 28, 641-648. (doi: 10.1111/j.1540-8175.2011.01406.x.)

Cerqueira, M.D., Weissman, N.J., Dilsizian, V., Jacobs, A.K., Kaul, S., Laskey, W.K., Pennell,D.J., Rumberger, J.A., Ryan, T. & Verani, M.S.. 2002. Standardized myocardial segmentation and nomenclature for tomographic imaging of the heart: a statement for healthcare professionals from the Cardiac Imaging Committee of the Council on Clinical Cardiology of the American Heart Association. Circulation, 105, 539-542. (doi: 10.1161/hc0402.102975)

Clarke, K.R. & Ainsworth, M. 1993. A method of linking multivariate community structure to environmental variables. Marine Ecology. Progress Series, 92, 205–219. (doi: 10.3354/meps092205)

Corno, A.F., Kocica, M.J. & Torrent-Guasp, F. 2006. The helical ventricular myocardial band of TorrenteGuasp: potential implications in congenital heart defects. European Journal of Cardiothoracic Surgery, 29, S61-S68.

D'Agostino, H.J. Jr, Pritchett, E.L., Shand, D.G. & Jones RH. 1983. Effect of verapamil on left ventricular function at rest and during exercise in normal men. Journal of Cardiovascular Pharmacology, 5, 812-817.

Evangelista, A., Nardinocchi, P., Puddu, P.E., Teresi, L., Torromeo, C. & Varano, V. 2011. Torsion of the human left ventricle: experimental analysis and computational modelling. Progress in Biophysics and Molecular Biology, 107, 112-121. (doi: 10.1016/j.pbiomolbio.2011.07.008)

Evangelista, A., Nesser, J., De Castro, S, Faletra, F., Kuvin, J., Patel, A., Alsheikh-Ali, A.A. & Pandian, N. 2009. Systolic wringing of the left ventricular myocardium: characterization of myocardial rotation and twist in endocardial and midmyocardial layers in normal humans employing three-dimensional speckle tracking study. Journal of the American College of Cardiology, 53 (Suppl. A239), 1018-268 (Abstr).

Geyer, H., Caracciolo, G., Abe, H., Wilansky, S., Carerj, S., Gentile, F., Nesser, H.J., Khandheria, B., Narula, J. & Sengupta, P.P. 2010. Assessment of myocardial mechanics using speckle tracking echocardiography: fundamentals and clinical applications. Journal of the American Society of Echocardiography, 23, 351-369. (doi: 10.1016/j.echo.2010.02.01)

Grosberg, A. & Gharib, M. 2009. Computational models of heart pumping efficiencies based on contraction waves in spiral elastic bands. Journal of Theoretical Biology, 257, 359-370. (doi: 10.1016/j.jtbi.2008.11.022)

Grosu, A., Bombardini, T., Senni, M., Duino, V., Gori, M. & Picano, E. 2005. End-systolic pressure/volume relationship during dobutamine stress echo: a prognostically useful non-invasive index of left ventricular contractility. European Heart Journal, 26, 2404-2412. (doi: 10.1093/eurheartj/ehi444)

Hansen, D.E., Daughters, G.T. 2nd, Alderman, E.L., Ingels, N.B., Stinson, E.B. & Miller, D.C. 1991. Effect of volume loading, pressure loading, and inotropic stimulation on left ventricular torsion in humans. Circulation, 83, 1315-1326. (doi: 10.1161/01.CIR.83.4.1315)

Higginbotham, M.B., Morris, K.G., Williams, R.S., McHale, P.A., Coleman, R.E.& Cobb, F.R. 1986. Regulation of stroke volume during submaximal and maximal upright exercise in normal man. Circulation Research, 58, 281-291. (doi: 10.1161/01.RES.58.2.281)

Jolliffe, I.T. 1982. A note on the Use of Principal Components in Regression. Journal of the Royal Statistical Society Series C, 31, 300–303. (doi:10.2307/2348005)

Kim, H.K., Sohn, D.W., Lee, S.E., Choi, S.Y., Park, J.S., Kim, Y.J., Oh, B.H., Park, Y.B. & Choi, Y.S. 2007. Assessment of left ventricular rotation and torsion with two-dimensional speckle tracking echocardiography. Journal ofthe American Society of Echocardiography, 20, 45-53. (doi: 10.1016/j.echo.2006.07.007)

Kim, W.J., Lee, B.H., Kim, Y.J., Kang, J.H., Jung, Y.J., Song, J.M., Kang, D.H. & Song, J.K. 2009. Apical rotation assessed by speckle-tracking echocardiography as an index of global left ventricular contractility. Circulation Cardiovascular Imging, 2, 123-131. (doi: 10.1161/CIRCIMAGING.108.794719)

Kleijn, S.A., Brouwer, W.P., Aly, M.F., Rüssel, I.K., de Roest, G.J., Beek, A.M., van Rossum, A.C. & Kamp, O. 2012. Comparison between three-dimensional speckle-tracking echocardiography and cardiac magnetic resonance imaging for quantification of left ventricular volumes and function. European Heart Journal Cardiovascular Imging, 13, 834-839. (doi: 10.1093/ehjci/jes030)

Lower, R. 1669. Tractatus de corde item de motu et colore sanguinis, et chyli in eum transitu. Amstelodami, apud Danielem Elzevirium 26-32.

Maffessanti, F., Nesser, H.J., Weinert, L., Steringer-Mascherbauer, R., Niel, J., Gorissen, W., Sugeng, L., Lang, R.M. & Mor-Avi, V. 2009. Quantitative evaluation of regional left ventricular function using three-dimensional speckle tracking echocardiography in patients with and without heart disease. American Journal of Cardiology, 104, 1755-1762. (doi: 10.1016/j.amjcard.2009.07.060)

Mitteroecker, P., Gunz, P., Neubauer, S., Müller, G. 2012. How to Explore Morphological Integration in Human Evolution and Development? Evolutionary Biology, 39, 536-553. (doi:10.1007/s11692-012-9178-3.)

Nardinocchi, P., Puddu, P.E., Teresi, L. & Varano, V. 2012. Advantages in the torsional performances of a simplified cylindrical geometry due to transmural differential contractile properties. European Journalof Mechanics A/Solids,36, 173-179. (doi: 10.1016/j.euromechsol.2012.03.001)

Nasiraei-Moghaddam, A. & Gharib, M. 2009. Evidence for the existence of a functional helical myocardial band. American Journal of Physiology-Heart and Circulatory Physiology, 296, H127-H131. (doi: 10.1152/ajpheart.00581.2008)

Nesser, H.J., Mor-Avi, V., Gorissen, W., Weinert, L., Steringer-Mascherbauer, R., Niel, J., Sugeng, L. & Lang, R.M. 2009. Quantification of left ventricular volumes using three-dimensional echocardiographic speckle tracking: comparison with MRI. European Heart Journal, 30, 1565-1573. (doi: 10.1093/eurheartj/ehp187)

Oksanen, J., Guillaume Blanchet. F,, Kindt, R., Legendre, P., Minchin, P.R., O'Hara, R.B., Simpson, G.L., Solymos, P., Henry, M., Stevens, H. & Wagner, H. 2013. vegan: Community Ecology Package. R package version 2.0-7.   http://CRAN.R-project.org/package=vegan

Park, S.M., Hong, S.J., Ahn, C.M., Kim, Y.H., Kim, J.S., Park, J.H., Lim, D.S. & Shim. W.J. 2012. Different impacts of acute myocardial infarction on left ventricular apical and basal rotation. European Heart Journal-Cardiovascular Imaging, 13, 483-489. (doi: 10.1093/ejechocard/jer272)

Pérez de Isla, L,, Balcones, D.V., Fernández-Golfín, C., Marcos-Alberca, P., Almería, C., Rodrigo, J.L., Macaya, C. & Zamorano J. 2009. Three-dimensional-wall motion tracking: a new and faster tool for myocardial strain assessment: comparison with two-dimensional-wall motion tracking. Journal of the American Society of Echocardiography, 22, 325-330. (doi: 10.1016/j.echo.2009.01.001) Erratum in: Journal of the American Society of Echocardiography 2009; 22, 745-e1.

Piras, P., Evangelista, A., Gabriele, S., Nardinocchi, P., Teresi, L., Torromeo, C., Schiariti, M., Varano, V., & Puddu, P.E. 2014. 4D-analysis of left ventricular heart cycle using Procrustes Motion Analysis. PLoS ONE 9(1): e86896. doi:10.1371/journal.pone.0086896

Puddu, P.E., Garlid, K.D., Monti, F., Iwashiro, K., Picard, S., Dawodu, A.A., Criniti, A., Ruvolo, G. & Campa,, P.P. 2000. Bimakalim: promising K_{ATP} channel activating agent. Cardiovascular Drug Reviews, 18, 25-46. (doi:10.1111/j.1527-3466.2000.tb00031.x)

R Core Team (2013). R: A language and environment for statistical   computing. R Foundation for Statistical Computing, Vienna, Austria. URL http://www.R-project.org/.

Rüssel, I.K., Götte, M.J., Bronzwaer, J.G., Knaapen, P., Paulus, W.J. & van Rossum, A.C. 2009. Left ventricular torsion: an expanding role in the analysis of myocardial dysfunction. Journal of the American College of Cardiology Cardiovascular Imaging, 2, 648-655. (doi: 10.1016/j.jcmg.2009.03.001)

Sagawa, K., Suga, H., Shoukas, A.A. & Bakalar, K.M. 1977. End-systolic pressure/volume ratio: a new index of ventricular contractility. American Journal of Cardiology, 40, 748-753. (doi: 10.1016/0002-9149(77)90192-8)

Sengupta, P.P., Korinek, J., Belohlavek, M., Narula, J., Vannan, M.A., Jahangir, A. & Khandheria, B.K. 2006. Left ventricular structure and function: basic science for cardiac imaging. Journal of the American College of Cardiology, 48, 1988-2001. (doi:10.1016/j.jacc.2006.08.030)

Sengupta, P.P., Tajik, A.J., Chandrasekaran, K. & Khandheria, B.K. 2008. Twist mechanics of the left ventricle: principles and application. Journal of the American College of Cardiology Cardiovascular Imaging, 1, 366-376. (doi: 10.1016/j.jcmg.2008.02.006)

Shaw, S.M., Fox, D.J. & Williams, S.G. 2008. The development of left ventricular torsion and its clinical relevance. International Journal of Cardiology, 130, 319-325. (doi: 10.1016/j.ijcard.2008.05.061)

Smerup, M., Nielsen, E., Agger, P., Frandsen, J., Vestergaard-Poulsen, P., Andersen, J., Nyengaard, J., Pedersen, M., Ringgaard, S., Hjortdal, V., Lunkenheimer, P.P. & Anderson, R.H. 2009. The three-dimensional arrangement of the myocytes aggregated together within the mammalian ventricular myocardium. Anatomical Records, 292, 1-11. (doi: 10.1002/ar.20798)

Streeter, D.D.Jr., Spotnitz, H.M., Patel, D.P., Ross, J.Jr. & Sonnenblick, E.H. 1969. Fiber orientation in the canine left ventricle during diastole and systole. Circulation Research, 24, 339–347.

Suga, H., Sagawa, K. & Shoukas, A.A. 1973. Load independence of the instantaneous pressure-volume ratio of the canine left ventricle and effects of epinephrine and heart rate on the ratio. Circulation Research, 32, 314-322. (doi: 10.1161/01.RES.32.3.314)

Sun, J.P., Lam, Y.Y., Wu, C.Q., Yang, X.S., Guo, R., Kwong, J.S., Merlino, J.D. & Yu, C.M. 2012. Effect of age and gender on left ventricular rotation and twist in a large group of normal adults - A multicenter study. International Journal of Cardiology, 167, 2215-2221. (doi: 10.1016/j.ijcard.2012.06.017)

Uznańska, B., Chrzanowski, L., Plewka, M., Lipiec, P., Krzemińska-Pakuła, M. & Kasprzak, J.D. 2008. The relationship between left ventricular late-systolic rotation and twist, and classic parameters of ventricular function and geometry. Kardiologia Polska, 66, 740-749.

Vendelin, M., Bovendeerd, P.H. & Arts, T. 2002. Optimizing ventricular fibers: uniform strain or stress, but not ATP consumption, leads to high efficiency. American Journal of Physiology- Heart and Circulatory Physiology, 283, H1072-H1081. (doi: 10.1152/ajpheart.00874.2001)

Zhou, Z., Ashraf, M., Hu, D., Dai, X., Xu, Y., Kenny, B., Cameron, B., Nguyen, T., Xiong, L. & Sahn, D.J. 2010. Three-dimensional speckle-tracking imaging for left ventricular rotation measurement: an in vitro validation study. Journal of Ultrasound Medicine, 29, 903-909.

Table 1. Descriptive statistics for original variables used in this study. As described in the text, all these variables were cleaned up by sex differences and divided by BSA before statistical analyses. Abbreviations: ESV: End-Systolic volume; BSA: body surface area; Rot_Base: Rotation Base (6 segments) (degrees); Rot_Med: Rotation Medium (6 segments) (degrees); Rot_Apex: Rotation Apex (4 segments) (degrees); R_global: Rotation global (degrees); Twist_Base: Twist Base (6 segments) (degrees); Twist_Med: Twist Medium (6 segments) (degrees); Twist_Apex: Twist Apex (4 segments) (degrees);T_global: Twist global (degrees); TORS_Base: Torsion Base (6 segments) (degrees/cm); TORS_Base :Torsion Medium (6 segments) (degrees/cm); TORS_Apex: Torsion apex (4 segments) (degrees/cm); TORS_globalTorsion Global (16 segments) (degrees/cm).

Acronim	n	Mean	Stand. Dev	Median	Min	Max	Range	Skew	Kurtosis	Stand. Err.
Sex	F=10; M=22	-	-	-	-	-	-	-	-	-
Age	32	34.94	11.71	30	21	60	39	1.03	-0.46	2.07
ESV	32	48.92	12.68	49.5	25	83	58	0.12	0.06	2.24
BSA	32	1.87	0.21	1.86	1.37	2.21	0.84	-0.4	-0.6	0.04
Rot_Base	32	0.02	2.51	0.18	-4.92	5.2	10.12	0.04	-0.59	0.44
Rot_Med	32	3.86	2.44	3.45	-0.86	8.84	9.7	0.23	-0.66	0.43
Rot_Apex	32	7.1	2.8	7.62	1.06	13.12	12.06	-0.11	-0.64	0.5
R_global	32	3.23	2.09	3.42	-1.19	7.3	8.49	-0.16	-0.92	0.37
Twist_Base	32	0.78	2.12	0.7	-3.46	6.74	10.2	0.65	0.67	0.38
Twist_Med	32	4.63	3.77	5.05	-3.93	12.02	15.95	-0.32	-0.37	0.67
Twist_Apex	32	7.85	3.47	7.84	2.04	16.55	14.51	0.4	-0.05	0.61
T_global	32	3.99	2.8	4.16	-0.9	9.78	10.68	0.17	-0.53	0.49
TORS_Base	32	0.42	1.7	0.32	-2.8	5.21	8.01	1.01	1.55	0.3
TORS_Med	32	1.15	1.11	1.33	-1.54	3.64	5.18	-0.28	0.07	0.2
TORS_Apex	32	1.31	0.61	1.34	0.33	3.28	2.95	0.82	1.5	0.11
TORS_global	32	0.91	1.13	0.94	-1.02	4.08	5.1	0.66	0.85	0.2

Table 2: Single Univariate Regressions between ESVI as Dependent and Torsional Parameters as Independents. in Bold Significant Values

	R-squared	Adj. R-squared	*p*-value
Rot_Base	0.16675	0.13897	**0.0228**
Rot_Med	0.00021	-0.03312	0.9384
Rot_Apex	0.03418	0.00199	0.3054
R_global	0.056	0.02453	0.195
Twist_Base	0.03096	-0.00134	0.337
Twist_Med	0.02868	-0.0037	0.351
Twist_Apex	0.00003	-0.0333	0.9762
T_global	0.00129	-0.032	0.8418
TORS_Base	0.05703	0.0256	0.1862
TORS_Med	0.00369	-0.02952	0.7436
TORS_Apex	0.01568	-0.01714	0.4972
TORS_global	0.01771	-0.01504	0.4642
TORS_global	0.01771	-0.01504	0.4642

Table 3. Summary Statistics for the PCA Performed on the Independent Table

	Standard Deviation	Proportion of Variance	Cumulative Variance
PC1	2.60900	0.56720	0.56720
PC2	1.71500	0.24510	0.81230
PC3	1.26700	0.13370	0.94600
PC4	0.74440	0.04618	0.99220
PC5	0.27200	0.00616	0.99830
PC6	0.11840	0.00117	0.99950
PC7	0.07458	0.00046	1.00000
PC8	0.01573	0.00002	1.00000
PC9	0.00873	0.00001	1.00000

Table 4. Summary Statistics for the Regression Model with ESVI as Dependent and Rotation Base as Independent. in Bold Significant Values

	Estimate	Standard error	t-value	*p*-value
Intercept	26.187	0.985	26.590	**<2e-16**
Beta	-2.010	0.820	-2.450	**0.020**
AIC	204.64			
Residual standard error (30 DF)	5.569			
Multiple R-squared	0.167			
Adjusted R-squared	0.139			
$F_{1,30}$	6.003			**0.020**

Table 5. Summary Statistics for the Regression Model with ESVI as Dependent and PC4 as Independent. in Bold Significant Values

	Estimate	Standard error	t-value	*p*-value
Intercept	26.104	0.811	32.183	**<2e-16**
Beta	-5.312	1.107	-4.799	**4.1e-5**
AIC	192.25			
Residual standard error (30 DF)	4.588			
Multiple R-squared:	0.434			
Adjusted R-squared:	0.415			
$F_{1,30}$ statistic:	23.03			**4.1e-5**

Table 6. Correlation Coefficients of Torsional Parameters with ESVI and PC4

	PC4	ESVI
Rot_Base	0.315	-0.408
Rot_Med	-0.347	0.014
Rot_Apex	0.063	-0.185
R_global	0.004	-0.237
Twist_Base	0.244	-0.176
Twist_Med	-0.295	0.169
Twist_Apex	-0.008	0.006
T_global	-0.080	0.036
TORS_Base	0.334	-0.239
TORS_Med	-0.186	0.061
TORS_Apex	0.111	-0.125
TORS_global	0.139	-0.133

Figure 1: 5-plane view as displayed by the Aplio-Artida 3D software: a) an apical 4-chamber view; b) a second apical view orthogonal to plane in a; C, 3, 5, 7) 3 short-axis planes: in the apical, midventricular and basal portions of the left ventricle, respectively

Figure 2: The results of the 3D analysis: a) 3D rotation shows the plastic bag of the left ventricle model freezed in endsystolic frame; b) Rotation (degrees) displays the averaged values for all 16 segments in each frame of the cardiac cycle and the time-curves graphs
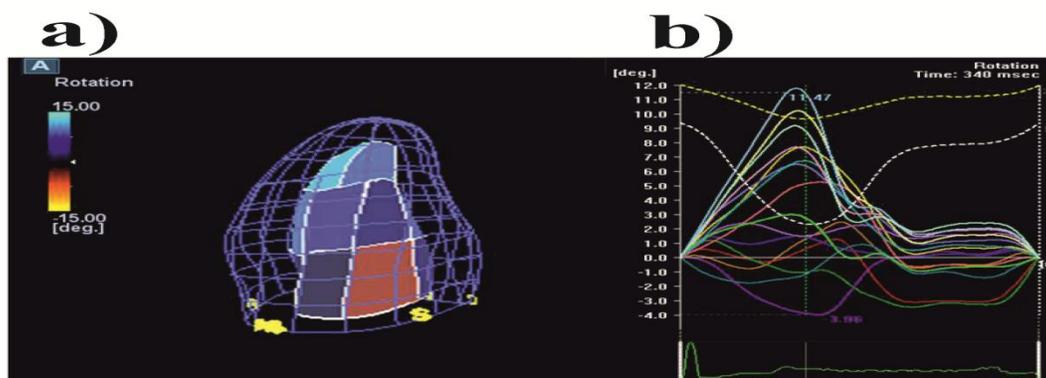
Figure 3: Scatterplot between ESVI (as dependent) and rotation_base (as independent). Regression line and confidence intervals are displayed. Summary statistics for this model are shown in Table 3. As described in the text, all measured variables were cleaned up by sex differences and divided by BSA before statistical analyses.
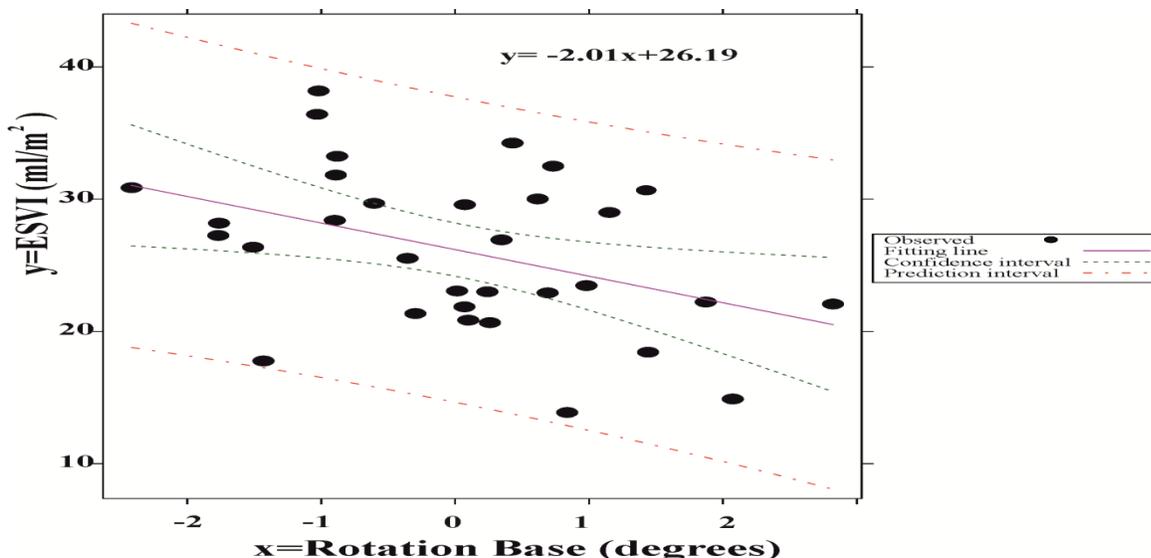
Figure 4. Scatterplot between ESVI (as dependent) and PC4 (as independent). Regression line and Confidence Intervals are displayed. Summary statistics for this model are shown in Table 4. As described in the text, all measured variables were cleaned up by sex differences and divided by BSA before statistical analyses.
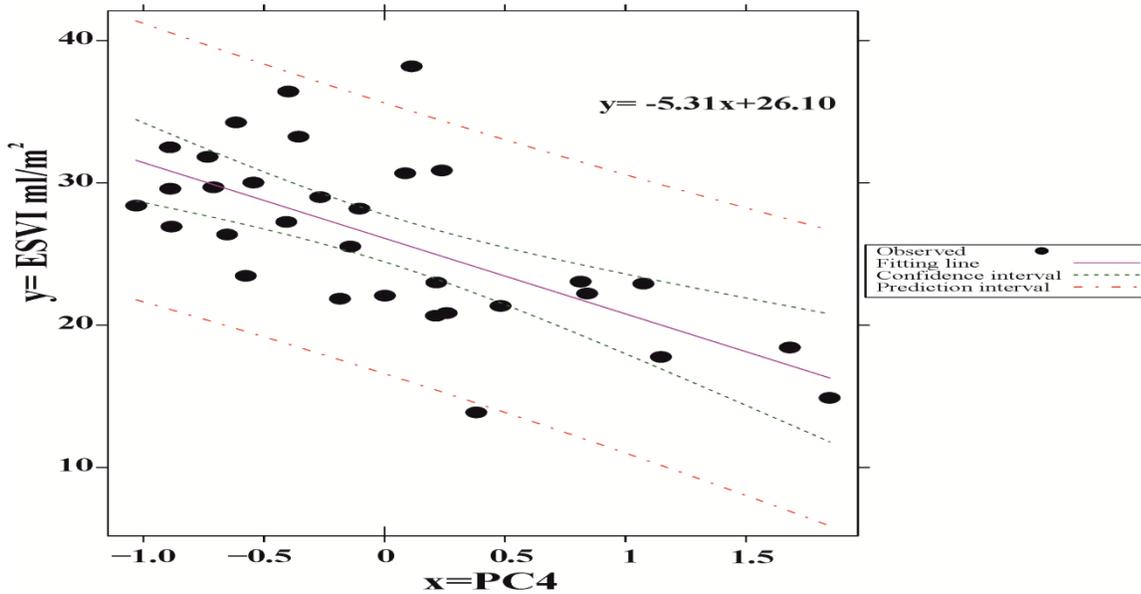
Figure 5. Correlation biplot between ESVI (as dependent) and PC4 (as independent) showing their correlation with original (BSA indexed and sex adjusted) torsional parameters. As described in the text, all measured variables were cleaned up by sex differences and divided by BSA before statistical analyses